AGU PUBLICATIONS

Geophysical Research Letters

RESEARCH LETTER
10.1002/2016GL068079

Key Points:
- Sunshade geoengineering to offset warming effect from $4 \times CO_2$ is simulated for a 1000 year period
- Throughout the 1000 year period, solar geoengineering leads to a climate state that is much closer to preindustrial than high-CO_2 world
- Throughout the 1000 year simulations, little climate drift is observed in the solar geoengineered world

Supporting Information:
- Supporting Information S1

Correspondence to:
L. Cao,
longcao@zju.edu.cn

Citation:
Cao, L., L. Duan, G. Bala, and K. Caldeira (2016), Simulated long-term climate response to idealized solar geoengineering, *Geophys. Res. Lett., 43*, 2209–2217, doi:10.1002/2016GL068079.

Received 2 FEB 2016
Accepted 25 FEB 2016
Accepted article online 1 MAR 2016
Published online 15 MAR 2016

Simulated long-term climate response to idealized solar geoengineering

Long Cao[1], Lei Duan[1], Govindasamy Bala[2], and Ken Caldeira[3]

[1]School of Earth Sciences, Zhejiang University, Hangzhou, China, [2]Divecha Center for Climate Change, Center for Atmospheric and Oceanic Sciences and Interdisciplinary Center for Water Research, Indian Institute of Science, Bangalore, India, [3]Department of Global Ecology, Carnegie Institution, Stanford, California, USA

Abstract Solar geoengineering has been proposed as a potential means to counteract anthropogenic climate change, yet it is unknown how such climate intervention might affect the Earth's climate on the millennial time scale. Here we use the HadCM3L model to conduct a 1000 year sunshade geoengineering simulation in which solar irradiance is uniformly reduced by 4% to approximately offset global mean warming from an abrupt quadrupling of atmospheric CO_2. During the 1000 year period, modeled global climate, including temperature, hydrological cycle, and ocean circulation of the high-CO_2 simulation departs substantially from that of the control preindustrial simulation, whereas the climate of the geoengineering simulation remains much closer to that of the preindustrial state with little drift. The results of our study do not support the hypothesis that nonlinearities in the climate system would cause substantial drift in the climate system if solar geoengineering was to be deployed on the timescale of a millennium.

1. Introduction

Increasing emissions of carbon dioxide from fossil fuel burning in recent decades have led to growing interest in using geoengineering as a potential means to counteract undesirable effects of global warming [*Keith*, 2000; *Crutzen*, 2006; *The Royal Society*, 2009; *Caldeira et al.*, 2013; *National Research Council*, 2015a, 2015b]. Geoengineering, which is the deliberate large-scale manipulation of the planetary environment to diminish the undesired effects of anthropogenic climate change [*Keith*, 2000], includes two categories of methods: carbon dioxide removal (CDR) and solar geoengineering, also known as solar radiation management (SRM) [*The Royal Society*, 2009] or albedo modification [*National Research Council*, 2015a]. CDR methods, by accelerating the removal of excess atmospheric CO_2, deal with a proximal cause of anthropogenic climate change. On the other hand, solar geoengineering methods aim to counteract anthropogenic warming by reducing the amount of sunlight reaching the Earth system. Because of its potential to cool the Earth rapidly at relatively low direct costs [*National Research Council*, 2015a], solar geoengineering has been a focus of research in the last decade.

Many modeling studies have investigated the effect of solar geoengineering on global climate. Simulations with direct reduction in solar irradiance have been widely used to examine climate response to idealized sunshade geoengineering scheme [e.g., *Govindasamy and Caldeira*, 2000; *Govindasamy et al.*, 2003; *Caldeira and Wood*, 2008; *Bala et al.*, 2008; *Lunt et al.*, 2008; *Irvine et al.*, 2009; *Kravitz et al.*, 2013; *Kalidindi et al.*, 2014]. Climate effects of stratospheric aerosol injection geoengineering are also being researched intensively [e.g., *Rasch et al.*, 2008; *Robock et al.*, 2008; *Jones et al.*, 2011; *Ferraro et al.*, 2011; *Niemeier et al.*, 2013; *Kalidindi et al.*, 2014]. These studies, in general, find that solar geoengineering is able to diminish a large part of CO_2-induced anthropogenic climate change, including surface warming, decline in Arctic sea ice, melting of Greenland ice sheet, and sea level rise. However, solar geoengineering is not able to restore a "natural" preindustrial climate for all regions and all climate fields. For example, if solar geoengineering is used to offset all CO_2-induced global mean warming, there will be a reduction in the global mean precipitation [e.g., *Bala et al.*, 2008; *Caldeira and Wood*, 2008; *Kravitz et al.*, 2013a; *Tilmes et al.*, 2013]. Recently, a set of standard solar geoengineering simulations were performed by multiple climate models as part of the Geoengineering Model Intercomparison Project x(GeoMIP) [*Kravitz et al.*, 2011, 2013a, 2013b]. These simulation experiments investigated climate response to geoengineering schemes including solar intensity reduction, stratospheric aerosol injection, and marine cloud brightening.

Most existing modeling studies on solar geoengineering have focused on climate consequence of solar geoengineering over timescales ranging from decades to a century. There is no peer-reviewed study

exploring millennial-scale implications of solar geoengineering. The National Research Council's report on solar geoengineering [*National Research Council*, 2015a] wrote, "Because the GeoMIP simulations are of limited duration (under a century), the deep ocean does not have time to come into equilibrium with the climate forcing. These G1 (simulations in which solar irradiance is reduced uniformly to offset warming effect from $4\times CO_2$) and $4\times CO_2$ simulations therefore do not provide an indication of how the climate would evolve if the albedo modification was maintained for centuries, allowing the deep ocean to respond …"

Our study attempts to address this issue identified by the National Research Council. One open question of interest is, if solar geoengineering was deployed long enough to allow for deep ocean to respond, would models predict that it would continue to be effective in counteracting anthropogenic climate change from elevated atmospheric CO_2 concentrations? This potential long-term need of solar geoengineering arises from long lifetime of anthropogenic CO_2, irreversibility of climate change on human time scales, and hence our long-term commitment to climate change. Elevated atmospheric CO_2 level and associated climate forcing would persist for millennia even if CO_2 emissions cease [*Archer et al*., 2009; *Eby et al*., 2009; *Gillett et al*., 2011; *Winkelmann et al*., 2015]. A multimodel intercomparison study [*Archer et al*., 2009] showed that in response to a 1000 (5000) Pg C CO_2 pulse emission, after 1000 years, about 10–30% (20–60%) CO_2 emission would remain in the atmosphere. Under the scenario of representative concentration pathways (RCPs 4.5–8.5) and their extensions, if anthropogenic CO_2 emissions were eliminated after year 2300, at year 3000, 85–99% of the maximum warming still remains and sea level continues rising [*Zickfeld et al*., 2013]. The long-term warming even after the elimination of anthropogenic CO_2 emission could also potentially lead to a collapse of the West Antarctic Ice Sheet [*Gillett et al*., 2011] as well as loss of nearly all of the East Antarctic Ice Sheet [*Winkelmann et al*., 2015], further contributing to large sea level rise. *McCusker et al*. [2015] found that in the scenario considered in their model, stratospheric aerosol injection did not effectively preserve the West Antarctic Ice Sheet because of continued upwelling of warm water that causes basal melting. As reported in the *National Research Council* [2015a], under the extended emission scenario of RCP 4.5, in the absence of further CO_2 emission reduction and large-scale deployment of CDR, solar geoengineering needs to be maintained to nearly year 2700 to keep CO_2-induced warming under 2°C. For the extended emission scenario of RCP 6.0, in the absence of further emission reduction and large-scale deployment of CDR, solar geoengineering needs to be maintained to year 3000 and beyond to keep CO_2-induced warming under 2°C.

In this study we examine long-term climate response to solar geoengineering over a time period up to a millennium. We use a coupled atmosphere-ocean climate model to perform long-term sunshade geoengineering simulation with a constant elevated atmospheric CO_2 level. We use this type of idealized simulation as the first attempt to understand long-term climate response to solar geoengineering, which was an unknown as emphasized in the *National Research Council* report [2015a].

2. Method

We use the UK Met Office Hadley Center climate model, HadCM3L [*Cox et al*., 2000], for this study. HadCM3L has a horizontal resolution of 3.75° longitude and 2.5° latitude for both the atmosphere and ocean with 19 nearly horizontal levels in the atmosphere and 20 horizontal levels in the ocean. The land component is represented by the MOSES II land surface scheme [*Essery and Clark*, 2003] with prescribed vegetation types and distributions. We first spun up the model for 3000 years under a constant atmospheric CO_2 concentration of 280 ppm and the default solar irradiance of 1365 W m^{-2} to obtain a quasi-equilibrium preindustrial climate state. Then, using the preindustrial climate state as the initial condition, three 1000 year simulations were performed: (1) a control simulation (CTR) with constant atmospheric CO_2 concentration of 280 ppm and the default solar irradiance of 1365 W m^{-2}; (2) a $4\times CO_2$ simulation in which atmospheric CO_2 is instantaneously quadrupled to 1120 ppm; (3) a SRM simulation in which atmospheric CO_2 is maintained at $4\times CO_2$ and at the same time solar irradiance is reduced by 4%. In HadCM3L a 4% reduction in solar irradiance approximately offsets global mean warming from $4\times CO_2$. This SRM simulation approximately mimics the effect of space-based sunshade geoengineering [*Angel*, 2006]. The three simulations performed here are of the similar design as the piControl, abrupt $4\times CO_2$, and the G1 experiment of GeoMIP [*Kravitz et al*., 2011], but with a much longer simulation period.

The overall departure of perturbed climate from preindustrial state can be measured in terms of root-mean-square (RMS) difference. Following the method of *Kravitz et al*. [2013a], we calculate the RMS difference for a climate variable between the simulation of $4\times CO_2$/SRM and CTR as

$$\mathrm{RMS}=\sqrt{\frac{\sum\left[\left(V_{\mathrm{exp}}-V_{\mathrm{ctr}}\right)^2 dA\right]}{\sum dA}} \tag{1}$$

where V_{exp} and V_{ctr} are annual mean values for a climate variable at a model grid from the experimental simulation ($4\times CO_2$ or SRM) and control simulation, respectively. dA is area of a model grid, and the summation is calculated for the entire globe, and separately for land and ocean. RMS difference defined in this way serves as a bulk measure of global climate departure from the control state.

3. Results

During the course of our 1000 year simulation, reduced solar irradiance offsets much of the global net energy imbalance at Top-of-Atmosphere (TOA) caused by increased atmospheric CO_2, leading to a global mean energy balance close to that of the control preindustrial state (Figure 1a). The maintenance of preindustrial TOA energy balance enables solar geoengineering to offset much of CO_2-induced warming throughout the 1000 year simulation period (Figures 1d–1f). Averaged over the latter half of the first century (years 60–100), the departure of global mean surface temperature in $4\times CO_2$ and SRM from CTR is 4.5 and 0.3 K, respectively. Averaged over the latter half of the last century (years 960–1000), the temperature departure in the $4\times CO_2$ simulation increases to 5.8 K but remains at 0.3 K for SRM (Figures 1d–1f and Table S1 in the supporting information).

During the 1000 year simulation period, elevated atmospheric CO_2 level increases global mean precipitation, and SRM causes a reduction in precipitation (Figure 1g). The decrease in global precipitation in SRM is a robust climate response in solar geoengineering simulations where solar irradiance reduction offsets CO_2-induced global mean warming [e.g., *Bala et al*., 2008; *Caldeira and Wood*, 2008; *Lunt et al*., 2008; *Kravitz et al*., 2013a]. As elucidated in previous studies [e.g., *Andrews et al*., 2009; *Cao et al*., 2012], this precipitation reduction is mainly a result of different fast precipitation response to CO_2 and solar forcing that develops prior to appreciable surface warming. Increased atmospheric CO_2 content increases stability of the lower atmosphere; this suppresses precipitation. In contrast, a change in solar intensity has little direct effect on precipitation (i.e., prior to the development of appreciable surface warming). In our simulation, SRM also prevents much of the sea ice melting throughout the 1000 year simulation period (Figure 1m). Specifically, in the $4\times CO_2$ simulation, global sea ice area shrinks by 42% and 58% for the periods of years 60–100 and 960–1000, respectively. For the same periods, simulated global sea ice area in SRM is only 6% and 4% less than that of the CTR (Table S1). Thus, the change in the amount of sea ice in the 900 years separating those two periods is 16% in the $4\times CO_2$ simulation but only 2% in the SRM simulation, indicating less climate drift in the SRM simulation.

Increased atmospheric CO_2 increases net primary production (NPP) mainly as a result of CO_2-fertilization effect, but the increase in NPP diminishes with time (Figure 1o) primarily because of increased surface temperature that imposes additional heat stress on the terrestrial biosphere. SRM, by reducing heat stress while maintaining the CO_2-fertilization effect, increases global NPP by a much larger amount than that of the $4\times CO_2$ (Figure 1o). We note that in our simulations, vegetation type and distributions are fixed, and there is no consideration of nutrient limitation. In addition, there are no changes to the fraction of direct to diffuse light nor aerosol-related ozone changes that could affect plant productivity. Therefore, cautions must be exercised in interpreting the simulated NPP response. Our 1000 year simulations are of much longer period than the GeoMIP simulations that last for only 50 years. Nevertheless, by comparing HadCM3L-simulated climate response during the first 50 years with that of corresponding GeoMIP simulations [*Kravitz et al*., 2013a], it is seen that HadCM3L-simulated climate change in response to $4\times CO_2$ and SRM is within the range of corresponding GeoMIP simulations (Table S2).

The simulated zonal and spatial patterns of climate change, including surface temperature, precipitation, precipitation minus evaporation ($P-E$), TOA and surface net energy flux balance, and NPP between $4\times CO_2$ and SRM are compared in Figures 2a–2c and S1–S5. There is little shift in the zonal and spatial

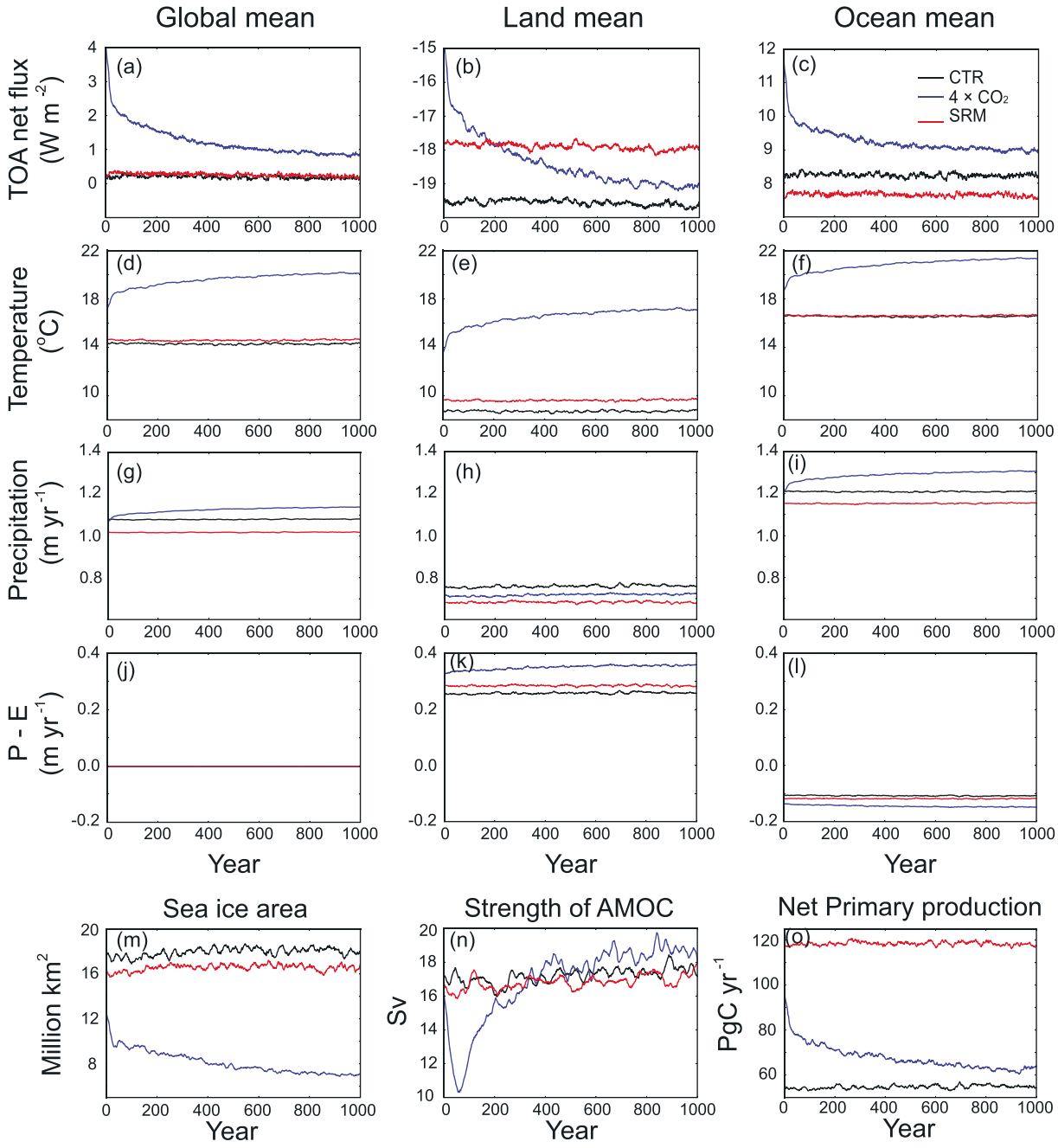

Figure 1. Model-simulated 1000 year time series for climate variables of (a–c) TOA net flux, (d–f) surface air temperature, (g–i) precipitation, (j–l) precipitation minus evaporation ($P - E$), (m) sea ice area, (n) maximum strength of Atlantic meridional circulation (AMOC), and (o) net primary production (NPP) in the simulation of CTR, $4 \times CO_2$, and SRM. A 20 year running averaging is applied to all variables.

patterns of simulated climate change in SRM between the latter half of the first century (years 60–100) and the latter half of the last century (years 960–1000). For example, throughout the 1000 year simulation, SRM causes an overcooling in the tropics and residual warming in the polar region (Figures 2a and S2) and a noted reduction in precipitation in the tropical region (Figures 2b and S3). In general, for both the first and last centuries, SRM leads to a global climate that is much more closer to CTR than is the $4 \times CO_2$ simulation.

The change in large-scale ocean circulation in response to solar geoengineering over several centuries has not been the focus of investigation in previous studies. In our simulations, in response to $4 \times CO_2$, the modeled strength of maximum Atlantic meridional overturning circulation (AMOC) decreases from its preindustrial value

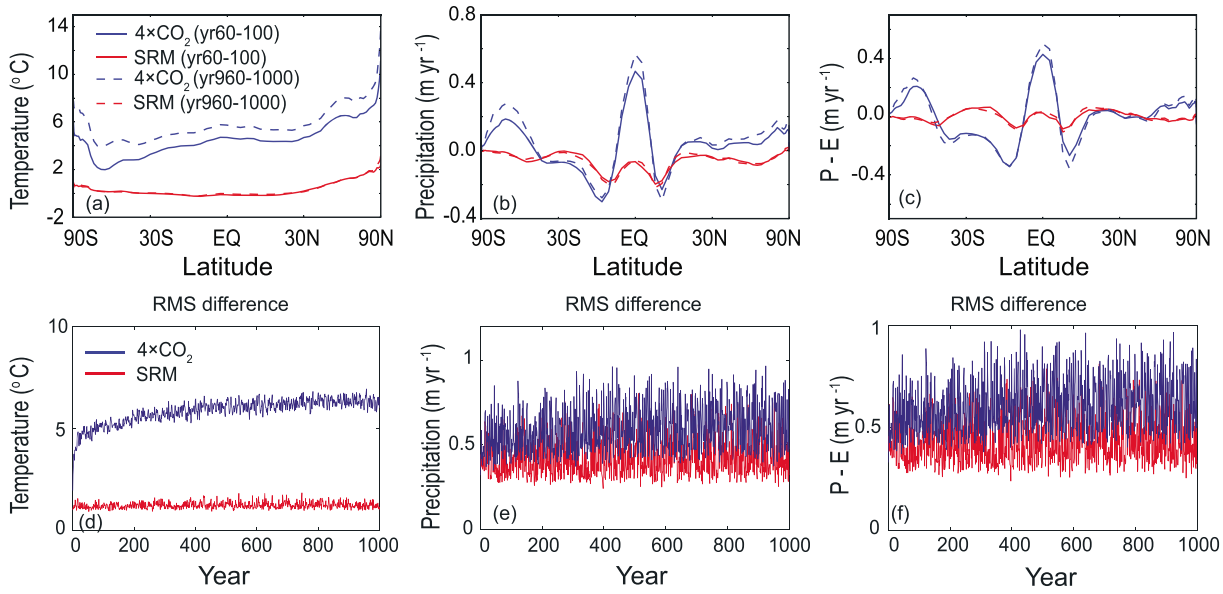

Figure 2. (a–c) Model-simulated zonal mean distribution of changes in surface air temperature, precipitation, and precipitation minus evaporation ($P - E$) in the $4 \times CO_2$ and SRM simulations for the period of years 60–100 and years 960–1000, respectively. Equal area is used in the X axis. (d–f) Temporal evolution of RMS difference in surface air temperature, precipitation, and precipitation minus evaporation ($P - E$) for the $4 \times CO_2$ and SRM simulations. RMS differences are calculated relative to the CTR simulation using equation (1) over the globe.

of 17.3 Sv (1 Sv = 10^6 m^3 s^{-1}) to a minimum value of 10.2 Sv by year 72 (Figure 1n). For comparison, *Lunt et al.* [2008], using 220 year HadCM3L simulations, reported a preindustrial AMOC strength of 18 Sv and a maximum AMOC reduction of 5 Sv in response to $4 \times CO_2$. As shown in Figure 1n, after the initial decrease in response to $4 \times CO_2$, simulated AMOC slowly recovers and eventually overshoots its preindustrial value. The initial weakening and gradual recovery of AMOC in response to increased atmospheric CO_2 concentration are common features found in many climate model simulations [e.g., *Stouffer and Manabe*, 1999; *Cheng et al.*, 2013; *Collins et al.*, 2013]. The initial weakening of AMOC is associated with increased surface temperature and freshwater flux at high latitude (Figures 2a, 2c, and S1), which reduces the density of surface water in the North Atlantic. *Gregory et al.* [2005] found that in 11 climate models, reduction in AMOC is caused more by the change in surface heat flux than change in freshwater flux. Over longer timescales, the simulated strength of AMOC starts to recover (Figure 1n), which would be an expected consequence of the gradual warming of subsurface water in low- and middle-latitude ocean [*Manabe and Stouffer*, 1994; *Stouffer and Manabe*, 1999] and increased northward salinity advection [*Thorpe et al.*, 2001; *Bitz et al.*, 2007]. A detailed analysis of the individual contribution to the reduction and recovery of AMOC, which requires additional simulations separating the role of heat and freshwater flux, is beyond the scope of this study. Nevertheless, HadCM3L-simulated AMOC change in response to $4 \times CO_2$ during the first 50 years is within the range of AMOC response from corresponding GeoMIP simulations (J. Moore, Beijing Normal University, personal communication, 2016).

In contrast to $4 \times CO_2$, throughout the 1000 year simulation, the intensity and pattern of AMOC show little change in our SRM simulation (Figures 1n and 3). During the 1000 year simulation period, the pattern of global meridional overturning circulation is much closer to CTR in the SRM simulation than in the $4 \times CO_2$ simulation (Figures 3 and S6), suggesting that SRM may be able to stabilize the Atlantic meridional overturning circulation on this time scale. The stabilization of AMOC in response to SRM can be explained by the stabilization of surface temperature and freshwater flux in the high-latitude oceans (Figures 2a, 2c, and S1). *Lunt et al.* [2008] reported that during the 220 year simulations, there is a slight increase in AMOC in response to SRM with a maximum increase of 1.6 Sv. In our 1000 year SRM simulation, relative to CTR, the change in AMOC ranges from −2.6 to 1.4 Sv with a mean anomaly of −0.3 and −0.2 Sv averaged over years 60–100 and 960–1000, respectively (Table S1). HadCM3L-simulated change of AMOC in response to SRM during the first 50 years is also within the range of AMOC response in corresponding GeoMIP G1 simulations (J. Moore, Beijing Normal University, personal communication, 2016). SRM also prevents warming of the deep ocean throughout the 1000 year simulation. Averaged over years 960–1000, in response to $4 \times CO_2$,

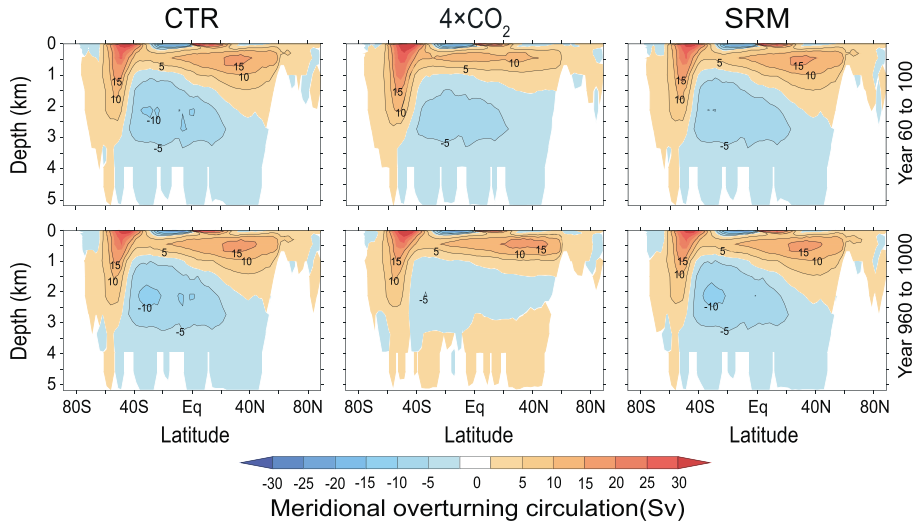

Figure 3. Model-simulated latitude-depth distribution of global ocean meridional overturning circulation for the CTR, $4 \times CO_2$, and SRM simulations. Time mean results are shown for the simulation period of years 60–100 and years 960–1000. The unit is sverdrup (Sv) ($1\ Sv = 10^6\ m^3\ s^{-1}$).

~3°C warming has penetrated to more than 2000 m, while in response to SRM, little warming in the deep ocean is simulated (Figure S7).

As shown in Figures 2d–2f and S8, throughout the 1000 year simulations, the RMS difference of temperature, precipitation, and $P - E$, relative to that of CTR, is smaller for the SRM than $4 \times CO_2$ simulation. For example, for surface temperature, the RMS difference in $4 \times CO_2$ relative to CTR keeps increasing with time, reaching 5.0 and 6.3 K (calculated over the globe) for years 60–100 and 960–1000, respectively. However, in SRM relative to CTR, the corresponding RMS difference remains at 0.8 K throughout the simulations (Table S3), indicating the ability of SRM to stabilize surface temperature at the global scale.

We also examine modeled climate change in $4 \times CO_2$ and SRM relative to the internal variability of CTR. To do this, we divide the modeled anomaly in a climate variable (relative to CTR) in $4 \times CO_2$ or SRM by the standard deviation (σ) of that variable calculated from the 1000 year time series of CTR. As shown in Figures 4, S9, and S10, compared to $4 \times CO_2$, during the 1000 year simulation period, SRM is effective in keeping simulated climate change, such as temperature, precipitation, and sea ice closer to the range typical of internal climate variability. For example, in SRM, averaged over periods of both years 60–100 and years 960–1000, ~90% area of the globe has surface temperature change less than 2σ of CTR (Table S4). In contrast, for $4 \times CO_2$, only 2% area of the globe has temperature change less than 2σ over years 60–100, and over years 960–1000, almost nowhere is temperature change less than 2σ (Table S4). As for precipitation, for SRM, almost all globe has change less than 2σ of CTR over periods of years 60–100 and years 960–1000. However, for $4 \times CO_2$, 80% and 71% area of the globe has change less than 2σ over years 60–100 and 960–1000, respectively (Table S4).

4. Discussion and Conclusions

Because of the slow natural processes to remove CO_2 from the atmosphere, unless anthropogenic CO_2 emission is reduced rapidly to near-zero values, substantial amount of atmospheric CO_2 and its climate forcing would persist for millennia. Theoretically, it may be possible to withdraw CO_2 from the atmosphere with CDR, but doing so would be technically and economically challenging [*National Research Council*, 2015b]. Given the long lifetime of anthropogenic CO_2, the effective irreversibility of climate change on human timescales and hence the long-term climate change commitment, solar geoengineering, if ever deployed in the absence of large-scale implementation of CDR schemes, might induce strong incentives to maintain the system for millennia [*National Research Council*, 2015a]. Earlier studies concluded that if anthropogenic CO_2 emissions were unabated and solar geoengineering were relied on to mitigate CO_2-induced warming, the consequences of geoengineering termination would engender increasing risk [*Matthews and Caldeira*,

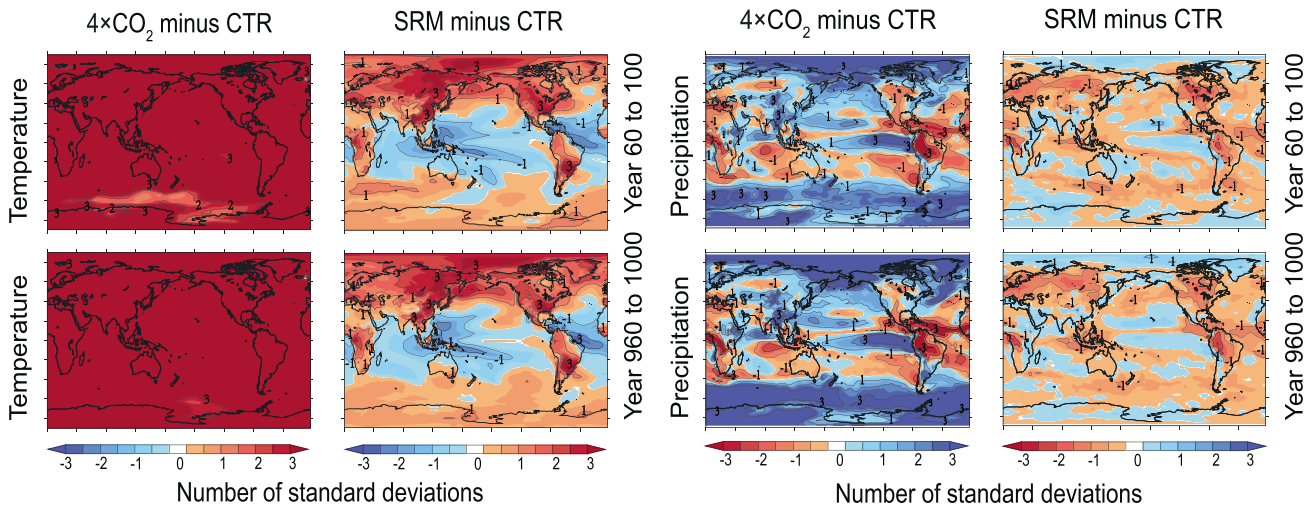

Figure 4. Model-simulated anomalies (relative to the CTR simulation) of surface air temperature and precipitation divided by the corresponding standard deviations for the CTR simulation. Anomalies are time mean results for the simulation period of years 60–100 and years 960–1000, respectively. Standard deviations are calculated from the 1000 year time series for the CTR simulation.

2007; *Brovkin et al*., 2009; *Jones et al*., 2013], providing additional incentive for continuous long-term solar geoengineering in the absence of mitigation and large-scale CDR deployment.

In this study, we assess the long-term climate response to solar geoengineering by performing a 1000 year simulation in which a uniform reduction in solar irradiance is used to offset CO_2-induced global warming. Our results suggest that solar geoengineering may be able to diminish many aspects of CO_2-induced climate change without substantial drift in geoengineered surface climate. If continued long-term climate change was to occur under long-term solar geoengineering, it would most likely arise from accumulated dynamic feedback of the ocean, which is one important aspect of the climate system that can undergo major changes on the centennial timescale. At time progresses, ice sheet response would also become important [*McCusker et al*., 2015]; climate feedbacks involving ice sheets are not addressed in this study. Our findings from simulations of a single climate model do not guarantee that long-term climate change would not occur in the real world if solar geoengineering was deployed over many centuries. Multimodel experiments, preferably with higher resolutions in the ocean, are needed to further investigate long-term climate response to solar geoengineering.

We have examined the long-term effect of solar geoengineering on some physical aspects of the climate system including temperature, hydrological cycle, sea ice, and large-scale ocean circulation. Other important elements of the climate system, including ice sheet, dynamic vegetation, the ocean and land carbon cycles, and marine and terrestrial ecosystems, are not included in the simulations here. It would be useful if these factors were explored in future studies. Also, here we assumed a constant $4\times CO_2$ stabilization concentration throughout the 1000 year simulations. A less simplistic scenario in the future could be that solar geoengineering is implemented to counteract climate change with gradual change in anthropogenic CO_2 emissions. In this context, geoengineered climate would depend on interactions between CO_2 emissions, atmospheric CO_2 concentration, and reduced solar irradiance. The long-term behavior of this coupled climate-carbon cycle system with solar geoengineering merits further study. Furthermore, we tested the long-term climate change in response to idealized sunshade geoengineering scheme; long-term climate and environmental response to other proposed solar geoengineering schemes, such as stratospheric aerosol injection and marine cloud brightening, is also a topic of investigation for future studies.

Our model simulations provide evidence that solar geoengineering may be capable of reducing effects from increased atmospheric greenhouse gas concentrations even on the 1000 year time scale. This is not a surprising result because the perturbation to air-sea energy fluxes is overall smaller in a high-CO_2 world with some appropriate amount of solar geoengineering than it would be without this solar geoengineering. Thus, ocean circulation would be expected to be less affected in the solar geoengineered high-CO_2 world than it would be in the high-CO_2 world in the absence of solar geoengineering. Because the $4\times CO_2$ simulation continues to

warm after the first century of simulation, whereas the solar geoengineering simulation does not have appreciable residual change, the difference between these two simulations grows appreciably with time. In contrast, the difference between the solar geoengineering simulation and the control simulation does not grow appreciably with time. Our results do not provide evidence that the degree of mismatch between the solar geoengineered climate and the preindustrial climate would increase over time if solar geoengineering were implemented continuously in a CO_2-stabilized world. Of course, the evidence we provide is limited and provisional and motivates further research aimed at assessing the robustness of our inferences. Furthermore, even in the absence of substantial residual climate drift, solar geoengineering deployed at large scale over a 1000 year interval would be a risky undertaking.

Acknowledgments

Long Cao and Lei Duan are supported by National Key Basic Research Program of China (2015CB953601), National Natural Science Foundation of China (41422503 and 41276073), and the Fundamental Research Funds for the Central Universities (2015XZZX004-05); Zhejiang University K. P. Chao's High Technology Development Foundation. Data are available upon request from the corresponding author (longcao@zju.edu.cn).

References

Andrews, T., P. M. Forster, and J. M. Gregory (2009), A surface energy perspective on climate change, *J. Clim.*, *22*, 2557–2570.

Angel, R. (2006), Feasibility of cooling the Earth with a cloud of small spacecraft near the inner Lagrange point (L1), *Proc. Natl. Acad. Sci. U.S.A.*, *103*, 17,184–17,189.

Archer, D., et al. (2009), Atmospheric lifetime of fossil fuel carbon dioxide, *Annu. Rev. Earth Planet. Sci.*, *37*, 117–134, doi:10.1146/annurev.earth.031208.100206.

Bala, G., P. B. Duffy, and K. E. Taylor (2008), Impact of geoengineering schemes on the global hydrological cycle, *Proc. Natl. Acad. Sci. U.S.A.*, *105*, 7664–7669, doi:10.1073/pnas.0711648105.

Bitz, C. M., J. C. H. Chiang, W. Cheng, and J. J. Barsugli (2007), Rates of thermohaline recovery from freshwater pulses in modern, Last Glacial Maximum, and greenhouse warming climates, *Geophys. Res. Lett.*, *34*, L07708, doi:10.1029/2006GL029237.

Brovkin, V., V. Petoukhov, M. Claussen, E. Bauer, D. Archer, and C. Jaeger (2009), Geoengineering climate by stratospheric sulfur injections: Earth system vulnerability to technological failure, *Clim. Change*, *92*, 243–259.

Caldeira, K., and L. Wood (2008), Global and Arctic climate engineering: Numerical model studies, *Philos. Trans. R. Soc. A*, *366*, 4039–4056, doi:10.1098/rsta.2008.0132.

Caldeira, K., G. Bala, and L. Cao (2013), The science of geoengineering, *Annu. Rev. Earth Planet. Sci.*, *41*, 231–256, doi:10.1146/annurev-earth-042711-105548.

Cao, L., G. Bala, and K. Caldeira (2012), Climate response to changes in atmospheric carbon dioxide and solar irradiance on the time scale of days to weeks, *Environ. Res. Lett.*, *7*, 034015, doi:10.1088/1748-9326/7/3/034015.

Cheng, W., J. C. H. Chiang, and D. Zhang (2013), Atlantic Meridional Overturning Circulation (AMOC) in CMIP5 models: RCP and historical simulations, *J. Clim.*, *26*, 7187–7197.

Collins, M., et al. (2013), Long-term climate change: Projections, commitments and irreversibility, in *Climate Change 2013: The Physical Science Basis. Contribution of Working Group I to the Fifth Assessment Report of the Intergovernmental Panel on Climate Change*, edited by T. F. Stocker et al., Cambridge Univ. Press, Cambridge, U. K., and New York.

Cox, P. M., R. A. Betts, C. D. Jones, S. A. Spall, and I. J. Totterdell (2000), Acceleration of global warming due to carbon-cycle feedbacks in a coupled climate model, *Nature*, *408*, 184–187.

Crutzen, P. J. (2006), Albedo enhancement by stratospheric sulfur injections: A contribution to resolve a policy dilemma?, *Clim. Change*, *77*, 211–220, doi:10.1007/s10584-006-9101-y.

Eby, M., K. Zickfeld, A. Montenegro, D. Archer, K. J. Meissner, and A. J. Weaver (2009), Lifetime of anthropogenic climate change: Millennial time scales of potential CO_2 and temperature perturbations, *J. Clim.*, *22*, 2501–2511.

Essery, R., and D. B. Clark (2003), Developments in the MOSES 2 land surface model for POLPS2e, *Global Planet. Change*, *38*, 161–164.

Ferraro, A. J., E. J. Highwood, and A. J. Charlton-Perez (2011), Stratospheric heating by potential geoengineering aerosols, *Geophys Res. Lett.*, *38*, L24706, doi:10.1029/2011GL049761.

Gillett, N., V. Arora, K. Zickfeld, S. Marshall, and W. Merryfield (2011), Ongoing climate change following a complete cessation of carbon dioxide emissions, *Nat. Geosci.*, *4*, 83–87.

Govindasamy, B., and K. Caldeira (2000), Geoengineering Earth's radiation balance to mitigate CO_2-induced climate change, *Geophys. Res. Lett.*, *27*, 2141–2144, doi:10.1029/1999GL006086.

Govindasamy, B., K. Caldeira, and P. B. Duffy (2003), Geoengineering Earth's radiation balance to mitigate climate change from a quadrupling of CO_2, *Global Planet. Change*, *37*(1–2), 157–168.

Gregory, J. M., et al. (2005), A model intercomparison of changes in the Atlantic thermohaline circulation in response to increasing atmospheric CO_2 concentration, *Geophys. Res. Lett.*, *32*, L12703, doi:10.1029/2005GL023209.

Irvine, P. J., D. J. Lunt, E. J. Stone, and A. Ridgwell (2009), The fate of the Greenland Ice Sheet in a geoengineered, high CO_2 world, *Environ. Res. Lett.*, *4*, 045109, doi:10.1088/1748-9326/4/4/045109.

Jones, A., J. Haywood, and O. Boucher (2011), A comparison of the climate impacts of geoengineering by stratospheric SO_2 injection and by brightening of marine stratocumulus cloud, *Atmos. Sci. Lett.*, *12*, 176–183, doi:10.1002/asl.29.

Jones, A., et al. (2013), The impact of abrupt suspension of solar radiation management (termination effect) in experiment G2 of the Geoengineering Model Intercomparison Project (GeoMIP), *J. Geophys. Res. Atmos.*, *118*, 9743–9752, doi:10.1002/jgrd.50762.

Kalidindi, S., G. Bala, A. Modak, and K. Caldeira (2014), Modeling of solar radiation management: A comparison of simulations using reduced solar constant and stratospheric sulphate aerosols, *Clim. Dyn.*, 1–17, doi:10.1007/s00382-014-2240-3.

Keith, D. W. (2000), Geoengineering the climate: History and prospect, *Annu. Rev. Energy Environ.*, *25*, 245–284, doi:10.1146/annurev.energy.25.1.245.

Kravitz, B., A. Robock, O. Boucher, H. Schmidt, K. E. Taylor, G. Stenchikov, and M. Schulz (2011), The Geoengineering Model Intercomparison Project (GeoMIP), *Atmos. Sci. Lett.*, *12*, 162–167, doi:10.1002/asl.316.

Kravitz, B., et al. (2013a), Climate model response from the Geoengineering Model Intercomparison Project (GeoMIP), *J. Geophys. Res. Atmos.*, *118*, 8320–8331, doi:10.1002/jgrd.50646.

Kravitz, B., et al. (2013b), Sea spray geoengineering experiments in the Geoengineering Model 20 Intercomparison Project (GeoMIP): Experimental design and preliminary results, *J. Geophys. Res. Atmos.*, *118*, 11,175–11,186, doi:10.1002/jgrd.50856.

Lunt D. J., A. Ridgwell, P. J. Valdes, and A. Seale (2008), 'Sunshade world': A fully coupled GCM evaluation of the climatic impacts of geoengineering, *Geophys. Res. Lett.*, *35*, L12710, doi:10.1029/2008GL033674.

Manabe, S., and R. J. Stouffer (1994), Multiple-century responses of a coupled ocean–atmosphere model to an increase of atmospheric carbon dioxide, *J. Clim.*, *7*, 5–23.

Matthews, H. D., and K. Caldeira (2007), Transient climate-carbon simulations of planetary geoengineering, *Proc. Natl. Acad. Sci. U.S.A.*, *104*(24), 9949–9954, doi:10.1073/pnas.0700419104.

McCusker, K. E., D. S. Battisti, and C. M. Bitz (2015), Inability of stratospheric sulfate aerosol injections to preserve the West Antarctic Ice Sheet, *Geophys. Res. Lett.*, *42*, 4989–4997, doi:10.1002/2015GL064314.

National Research Council (2015a), *Climate Intervention: Reflecting Sunlight to Cool Earth*, pp. 234, National Academies Press, Washington, D. C.

National Research Council (2015b), *Climate Intervention: Carbon Dioxide Removal and Reliable Sequestration*, 140 pp., National Academies Press, Washington, D. C.

Niemeier, U., H. Schmidt, K. Alterskjær, and J. E. Kristjánsson (2013), Solar irradiance reduction via climate engineering: Impact of different techniques on the energy balance and the hydrological cycle, *J. Geophys. Res. Atmos.*, *118*, 11,905–11,917, doi:10.1002/2013JD020445.

Rasch, P. J., et al. (2008), An overview of geoengineering of climate using stratospheric sulphate aerosols, *Phil. Trans. R. Soc. A*, *366*, 4007–4037, doi:10.1098/rsta.2008.013.

Robock A., L. Oman, and G. L. Stenchikov (2008), Regional climate responses to geoengineering with tropical and arctic SO_2 injections, *J. Geophys. Res.*, *113*, D16101, doi:10.1029/2008JD010050.

Stouffer, R. J., and S. Manabe (1999), Response of a coupled ocean–atmosphere model to increasing atmospheric carbon dioxide: Sensitivity to the rate of increase, *J. Clim.*, *12*, 2224–2237.

The Royal Society (2009), *Geoengineering the Climate: Science, Governance and Uncertainty*, pp. 98, GB, Royal Society, London.

Thorpe, R. B., J. M. Gregory, T. C. Johns, R. A. Wood, and J. F. B. Mitchell (2001), Mechanisms determining the Atlantic thermohaline circulation response to greenhouse gas forcing in a non-flux-adjusted coupled climate model, *J. Clim.*, *14*, 3102–3116.

Tilmes, S., et al. (2013), The hydrological impact of geoengineering in the Geoengineering Model Intercomparison Project (GeoMIP), *J. Geophys. Res. Atmos.*, *118*, 11,036–11,058, doi:10.1002/jgrd.50868.

Winkelmann, R., A. Levermann, A. Ridgwell, and K. Caldeira (2015), Combustion of available fossil fuel resources sufficient to eliminate the Antarctic Ice Sheet, *Sci. Adv.*, E1500589.

Zickfeld, K., et al. (2013), Long-term climate change commitment and reversibility: An EMIC intercomparison, *J. Clim.*, *26*, doi:10.1175/JCLI-D-12-00584.1.